Int. J. Nano Dimens., 7(4): 284-289, Autumn 2016

ORIGINAL ARTICLE

Density functional explorations of quadrupole coupling constants for BN, BP, AlN, and AlP graphene–like structures

Mahmoud Mirzaei [1,*]; *Rahman Salamat Ahangari* [2]

[1] *Bioinformatics Research Center, Department of Medicinal Chemistry, School of Pharmacy and Pharmaceutical Sciences, Isfahan University of Medical Sciences, Isfahan, Iran*

[2] *Department of Chemistry, Faculty of Basic Sciences, Azarbaijan Shahid Madani University, Tabriz, Iran*

Received 11 January 2016; revised 13 April 2016; accepted 29 April 2016; available online 21 July 2016

Abstract

Stabilizations and atomic level quadrupole coupling constant (C_Q) properties have been investigated for graphene–like monolayers (G–monolayers) of boron nitride (BN), boron phosphide (BP), aluminum nitride (AlN), and aluminum phosphide (AlP) structures. To this aim, density functional theory (DFT) calculations have been performed to optimize the model structures and also to evaluate the C_Q parameters. The results of optimizations indicated that the formations, polarities, and semiconducting properties of BN G–monolayer are more favorable than other investigated G–monolayers. Moreover, the atomic level C_Q parameters also indicated that the atoms at the tips of monolayers have the most activities among other atoms and different properties have been seen for the atoms at different positions of monolayers. Differences of electronegativities are also important for the magnitudes of C_Q properties as could be seen by larger values of C_Q parameters for B and Al atoms in the BN and AlN G–monolayers in comparison with BP and AlP G–monolayers.

Keywords: *Aluminum; Boron; Density functional theory (DFT); Graphene; Nitrogen; Phosphorus.*

How to cite this article

Mirzaei M. Density functional explorations of quadrupole coupling constants for BN, BP, AlN, and AlP graphene–like structures. Int. J. Nano Dimens., 2016; 7 (4): 284-289, DOI: 10.7508/ijnd.2016.04.003

INTRODUCTION

The pioneering introductory of carbon nanotubes (CNTs) by Iijima [1] has raised intensive interests of researchers to investigate properties of this novel material and also to find possibilities of existence for other related nanostructures [2, 3]. The efforts have led to syntheses and characterizations of other nanostructures in addition to CNTs, in which graphene (G) has been introduced as a honeycomb monolayer of carbon atoms with wide surface area [4, 5]. The G-monolayers could be either extracted from graphite–multilayers or directly synthesized as outstanding structures [6, 7]. Considerable efforts have been also dedicated to characterize various aspects of G-monolayers through computations and experiments [8 – 10]. The surface of G–monolayer is expected to be proper for several applications in the field of surface sciences from biological systems and drug deliveries up to environmental applications and pollutant removals [11, 12]. However, the hydrophobic nature of G-monolayer makes this structure as an improper material for applications in the hydrated media [13]. Therefore, further investigations have been oriented to find nanostructures based on other atoms rather than carbon atoms. To this aim, combinations of atoms of third and fifth groups of elements (III–A and V–A) have been considered as possible substitutions for carbon nanostructures [14, 15]. Since the electronegativities of atoms of III–A and V–A are different, the new nanostructures could be also considered as ionic ones more proper for hydrated systems in comparison with non–ionic carbon nanostructures [16]. Possibilities of combinations of boron (B) and aluminum (Al) atoms of III–A with nitrogen (N) and phosphorous (P) atoms of V–A have been very well investigated through computation and experiments [17 – 20]. Stabilities and properties for tubular, conical, and planar models of BN, BP,

* Corresponding Author Email: *mdmirzaei@pharm.mui.ac.ir*

AlN, and AlP nanostructures have been reports by earlier studies [21-24]. Specifically, the stabilities and properties for combinations of B/Al and N/P atoms to construct nanocones have been earlier investigated through quantum computations [21]. Regarding electronic transferring properties, in which the carbon nanostructures are metals or semiconductors dependent on their structural properties, the III–V nanostructures have been seen as always semiconductors [25]. This character very well distinguishes the III–V nanostructures for specific purposes in electronic systems technologies instead of carbon nanostructures [26]. The ionic III–V surfaces could make possible several selective absorptions of external materials on the surfaces or they could be proper surfaces to catalyze chemical reactions in desired directions [27].

Within this work, stabilities and properties of molecular systems of BN, BP, AlN, and AlP G–monolayers (Fig. 1) have been investigated by advantages computational chemistry for characterizations at atomic and molecular level properties. Molecular systems with similar stoichiometries have been constructed for the investigated III–V models to be optimized to reach the minimum–energy structures. Molecular properties such as dipole moments and different types of energies have been evaluated by the results of optimization processes. Atomic level properties of quadrupole coupling constants (C_Q) have been also evaluated for the atoms of optimized structures to better examine the properties of investigated models at the atomic levels. It is really an advantage of computational chemistry to reproduce complicated spectroscopic parameters especially for complex systems

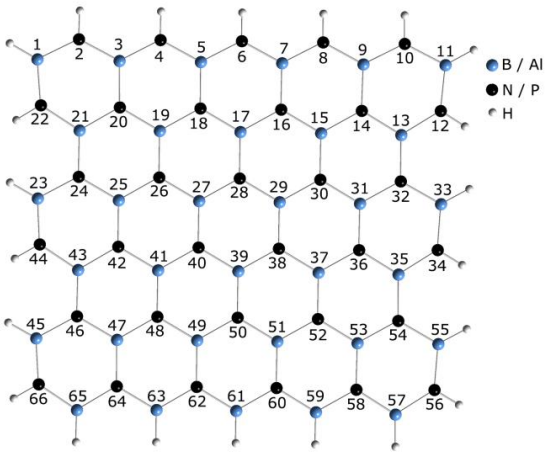

Fig. 1: 2D view of investigated III–V G–monolayers.

of nanostructures [28]. C_Q properties could be measured by solid–state nuclear magnetic resonance (NMR) spectroscopy, which are among the most versatile techniques of materials characterizations [29].

Since the electronic sites of atoms are origins for C_Q properties, they could very well reveal insightful information about the atomic structures of molecular systems. Using these advantages, the stabilities and properties for III–V models of this work including BN, BP, AlN, and AlP G–monolayers (Fig. 1) have been investigated through computations of molecular and atomic properties (Tables 1 and 2).

EXPERIMENTAL

Calculation

Electronic and structural properties for four monolayer models consisting of B and Al atoms of III–A group and N and P atoms of V–A group with the stoichiometries of $III_{33}V_{33}H_{22}$ (Fig. 1) have been investigated within this work. It is worth to mention that the role of hydrogens is to saturate the valance shells of atoms at the planar edges to mimic sp^2 hybridizations for them [30]. The models have been optimized to achieve the minimum energy level structures to find proper geometries for investigations of electronic and structural properties. Additionally, molecular properties including dipole moment (D_m), total energies (E_t), binding energies (E_b), and energy gaps (E_g) have been evaluated for the stabilized models by optimization processes (Table 1). D_m implies for the orientations of electronic distribution in the molecular structure and E_t implies for the energy of whole structure. E_b implies for the energy differences between the molecules and constructing atoms; $E_b = E(III_{33}V_{33}H_{22}) - 33E_{(III)} - 33E_{(V)} - 22E_{(H)}$. E_g implies for the energy differences of the highest occupied and the lowest unoccupied molecular orbiatls (HOMO and LUMO); $E_g = E_{HOMO} - E_{LUMO}$. In addition to optimized properties, atomic–scale properties of quadrupole coupling constants (C_Q) have been evaluated for the optimized structures to further analyze the properties of investigated models (Table 2). To this aim, electric field gradient (EFG) tensors have been calculated for the atoms of optimized structures to evaluate C_Q parameters; $C_Q = e^2Qq_{zz}h^{-1}$ [31]. The components e, Q, q_{zz}, and h are electric charge, nuclear electric quadrupole moment, main eigenvalue of EFG tensors, and Planck's constant [29]. It is noted that the C_Q

parameters could be obtained for those atoms with nuclear spin angular momentum (I) greater than one or equal to it; therefore, all atoms are not detectable by these parameters [29]. Accordingly, C_Q parameters have been obtained for B, Al, and N atoms of investigated models but not for P atoms (Table 2). All calculations have been performed at the level of density functional theory (DFT) using the B3LYP exchange–correlation functional and the 6–31G* standard basis set as implemented in the Gaussian 98 program [32].

RESULTS AND DISCUSSION

Optimized properties

The obtained values of optimized molecular properties for the BN, BP, AlN, and AlP G–monolayers (Fig. 1) of this work are summarized in Table 1. The values of dipole moments (D_m) indicate the levels of polarity as D_m(BN) > D_m(BP) > D_m(AlN) > D_m (AlP) showing the highest polarity for BN and the lowest one for AlP G–monolayers. The polarities are arisen because of different electronegativities of III–V hetero–structures whereas the value of dipole moment is almost zero for the original C homo–atomic monolayer [9]. It is important to note that the summations of atomic numbers for B and N atoms equals to the summations of atomic numbers for two C atoms; therefore, the BN structures are always considered as proper substitutions for the C structures. The values of total energies (E_t) do not directly show a remarkable trend; however, the binding energies (E_b) could show that the formation of BN G–monolayer is better achievable than other three BP, AlN, and AlP models, in which the formation of AlP G–monolayer is the worst achievable structure among the models. The formations for BP and AlN are almost similar to each other between the formations of BN and AlP G–monolayers. The electronic conductivity properties have been explored by the evaluations of energy gaps (E_g) for the investigated III–V G–monolayers. The results indicate that the BN G–monolayer shows the best semi–conducting property among the considered models. It is remembered that the III–V nanostructures are expected to show always semiconducting properties, in which the results of obtained E_G parameters show the expected semiconducting properties for all of four investigated models. In addition to very well behaved BN G–monolayer for semiconducting property, the other three models also show reasonable values of E_g to be categorized for semiconductors. As a result of this section, it could be mentioned that the formations of BN, BP, AlN, and AlP G–monolayers could be possible according to the obtained values of E_b for them. Moreover, different polarities indicated that the III–V structures could play different roles for dispersions in water media. Finally, the expected semiconducting property has been approved for the investigated III–V G–monolayers according to their values of Eg. Comparing the results of this work with earlier studies [18, 20, 21, 30] indicates that the properties of III–V nanostructures could be tuned through substitution of B by Al or N by P for the specific purposes of applications.

Quadrupole coupling constants

The values of quadrupole coupling constants (C_Q) for the B, N, and Al atoms of optimized BN, BP, AlN, and AlP G–monolayers (Fig. 1) are listed in Table 2. As mentioned earlier, because of isotopes abundances in nature, C_Q properties could be evaluated for B, Al, and N atoms but not for P atoms [29]. The results are showing the electronic properties of constructing atoms of investigated monolayers, which are important for the careful examinations of electronic structures of matters. For B and Al atoms, the structure could be divided into some atomic layers based on similarities of properties for atoms of that layer. According to Fig. 1, atoms III_1 to III_{11}, III_{13} to III_{21}, III_{23} to III_{33}, III_{35} to III_{43}, III_{45} to III_{55}, and III_{57} to III_{65} make their atomic layers

Table 1: Optimized structural properties for III–V graphenes *

Property	BNG	BPG	AlNG	AlPG
Stoichiometry	$B_{33}N_{33}H_{22}$	$B_{33}P_{33}H_{22}$	$Al_{33}N_{33}H_{22}$	$Al_{33}P_{33}H_{22}$
D_m /Debye	3.928	3.643	3.209	0.422
E_t /keV	–71.946	–329.235	–267.326	–524.654
E_b /eV	490.355	347.990	364.370	259.956
E_g /eV	5.945	2.461	4.760	3.776

* See Fig. 1 for details. (Dm: Dipole moment; Et: Total energy; Eb: Binding energy; Eg: Energy gap)

Table 2: B /Al / N quadrupole coupling constants (CQ /MHz) for III–V G–monolayers *

Atom	BN	BP	AlN	AlP	Atom	BN	AlN
B / Al 1	3.135	2.627	26.751	22.195	N 2	2.128	2.224
B / Al 3	2.652	1.897	23.504	15.983	N 4	2.361	2.303
B / Al 5	2.654	1.891	23.563	15.987	N 6	2.375	2.311
B / Al 7	2.654	1.891	23.563	15.987	N 8	2.361	2.303
B / Al 9	2.652	1.897	23.504	15.983	N 10	2.128	2.224
B / Al 11	3.135	2.627	26.751	22.195	N 12	1.753	2.058
B / Al 13	2.784	2.035	24.057	16.725	N 14	0.401	0.066
B / Al 15	2.832	2.003	24.292	16.823	N 16	0.433	0.049
B / Al 17	2.831	1.980	24.304	16.818	N 18	0.433	0.049
B / Al 19	2.832	2.003	24.292	16.823	N 20	0.401	0.066
B / Al 21	2.784	2.035	24.057	16.725	N 22	1.753	2.058
B / Al 23	3.248	2.752	27.255	22.994	N 24	0.257	0.149
B / Al 25	2.822	2.010	24.303	16.953	N 26	0.333	0.086
B / Al 27	2.849	2.035	24.376	17.040	N 28	0.318	0.095
B / Al 29	2.849	2.035	24.376	17.040	N 30	0.333	0.086
B / Al 31	2.822	2.010	24.303	16.953	N 32	0.257	0.149
B / Al 33	3.248	2.752	27.255	22.994	N 34	1.713	2.054
B / Al 35	2.828	2.106	24.228	17.019	N 36	0.301	0.085
B / Al 37	2.863	2.081	24.438	17.178	N 38	0.295	0.108
B / Al 39	2.862	2.043	24.492	17.194	N 40	0.295	0.108
B / Al 41	2.863	2.081	24.438	17.178	N 42	0.301	0.085
B / Al 43	2.828	2.106	24.228	17.019	N 44	1.713	2.054
B / Al 45	3.300	2.890	27.371	23.307	N 46	0.188	0.158
B / Al 47	2.864	2.133	24.361	17.293	N 48	0.267	0.102
B / Al 49	2.896	2.164	24.548	17.501	N 50	0.240	0.122
B / Al 51	2.896	2.164	24.548	17.501	N 52	0.267	0.102
B / Al 53	2.864	2.133	24.361	17.293	N 54	0.188	0.158
B / Al 55	3.300	2.890	27.371	23.307	N 56	1.746	2.101
B / Al 57	3.428	2.985	27.744	23.549	N 58	0.252	0.359
B / Al 59	3.604	3.228	28.300	24.307	N 60	0.252	0.440
B / Al 61	3.620	3.247	28.340	24.359	N 62	0.252	0.440
B / Al 63	3.604	3.228	28.300	24.307	N 64	0.252	0.359
B / Al 65	3.428	2.985	27.744	23.549	N 66	1.746	2.101

* See Fig. 1 for the numbers. (CQ: Quadrupole coupling constant)

as could be seen by the evidences of similarities for properties of atoms in the layers. As could be seen in Table 2, the obtained C_Q properties are the same for pairs of 1 and 11, 3 and 9, and 5 and 7 atoms for the first atomic layer.

Parallel results are also observed for the atoms of other layers. Similar results are also obtained for N atoms as could be seen by the magnitudes of C_Q parameters for atoms pairs of N_2 and N_{10}, N_4 and N_8 in the first atomic layer. The atomic layers based on the similarities of properties for atoms of each layer are categorized for N atoms as N_2 to N_{10}, N_{12} to N_{22}, N_{24} to N_{32}, N_{34} to N_{44}, N_{46} to N_{54}, and N_{56} to N_{66} layers. Careful examinations of magnitudes of C_Q parameters for constructing atoms indicate that the values for B atoms are larger in BN than BP G–monolayer. For Al atoms, the magnitudes of C_Q parameters are larger in AlN than AlP G–monolayer. This trend is because of differences of electronegativities between the atoms in III–V bonds. The order of electronegativities for investigated atoms is N > P > B > Al. Because of larger electronegativity differences between B – N and Al – N in comparison with B – P and Al – P, the obtained C_Q properties for B and Al atoms are larger in III–N than III–P G–monolayers. The magnitudes of C_Q for N atoms are almost similar to each other in BN and AlN monolayers.

Focusing on the magnitudes of C_Q parameters in each model indicates that the largest magnitudes for all B, Al, and N atoms are observed when they are located at the tip of monolayer, III_{57} – III_{65} and N_2 – N_{10} atoms. In other positions, the magnitudes of C_Q parameters are changed due to being in different chemical environments inside the monolayers. The results also indicate that the molecular properties are almost complicated by seeing so many differences of properties in

atomic levels investigations. Larger or smaller magnitudes for C_Q parameters of one atomic type are related to the magnitude of q_{zz} eigenvalue which is important for definition of capability of one atom for interactions with other atoms or molecules. Increasing the amount of electronic charges on one atom could encourage it for more interacting activities. Within our results, the most activities could be expected for atoms at the tips of G–monolayers in agreement with earlier trends on BN nanotubes [33].

CONCLUSION

DFT calculations have been performed to evaluate C_Q properties for the stabilized models of BN, BP, AlN, and AlP G–monolayers. The optimized molecular results indicated that the possibility of formations for BN G–monolayer is the most favorable among considered systems. Moreover, better polarities and semiconducting properties have been seen for the BN G–monolayer in comparison with other III–V G–monolayers. Atomic level C_Q parameters also indicate that the atoms of G–monolayers could be divided into atomic layers based on similarities of properties for atoms of each layer. Moreover, the atoms located at planar tips are activated more than the atoms of inner positions due to their larger magnitudes of C_Q parameters. Interestingly, larger differences of electronegativities yield larger magnitudes of C_Q parameters as could be seen for B and Al atoms in the III–N models comparing to the III–V models.

ACKNOWLEDGEMENTS

All supports for this work by the Research Council of Isfahan University of Medical Sciences are gratefully acknowledged.

CONFLICT OF INTEREST

The authors declare that there is no conflict of interests regarding the publication of this manuscript.

REFERENCES

[1] Iijima S., (1991), Helical microtubules of graphitic carbon. *Nature.* 354: 56-58.
[2] Ghorbanzadeh Ahangari M., Ganji M. D., Montazar F., (2015), Mechanical and electronic properties of carbon nanobuds: First–principles study. *Solid State Commun.* 203: 58-62.
[3] Shahgaldi S., Hamelin J., (2015) Improved carbon nanostructures as a novel catalyst support in the cathode side of PEMFC: a critical review. *Carbon.* 94: 705-728.
[4] Geim A. K., Novoselov K. S., (2007), The rise of graphene. *Nature Mater.* 6: 183-191.
[5] Geim A. K., (2009), Graphene: status and prospects. *Science.* 324: 1530-1534.
[6] Avouris P., Dimitrakopoulos C., (2012), Graphene: Synthesis and applications. *Mater. Today.* 15: 86–97.
[7] Sadasivuni K. K., Ponnamma D., Thomas S., Grohens Y., (2014), Evolution from graphite to graphene elastomer composites. *Prog. Polym. Sci.* 39: 749-780.
[8] Chatterjee S. G., Chatterjee S., Ray A. K., Chakraborty A. K., (2015), Graphene–metal oxide nanohybrids for toxic gas sensor: A review. *Sens. Actuat. B.* 221: 1170-1181.
[9] Rahimnejad S., Mirzaei M., (2011), Computational studies of planar, tubular and conical forms of silicon nanostructures. *Int. J. Nano. Dimens.* 1: 257-260.
[10] Prezhdo O. V., Kamat P. V., Schatz G. C., (2011), Virtual issue: graphene and functionalized graphene. *J. Phys. Chem. C.* 115: 3195-3197.
[11] Mianehrow H., Moghadam M. H. M., Sharif F., Mazinani S., (2015), Graphene–oxide stabilization in electrolyte solutions using hydroxyethyl cellulose for drug delivery application. *Int. J. Pharm.* 484: 276-282.
[12] Hua Z., Tang Z., Bai X., Zhang J., Yu L., Cheng H., (2015), Aggregation and resuspension of graphene oxide in simulated natural surface aquatic environments. *Environ. Pollut.* 205: 161-169.
[13] Konios D., Stylianakis M. M., Stratakis E., Kymakis E., (2014), Dispersion behavior of graphene oxide and reduced graphene oxide. *J. Colloid Interface Sci.* 430: 108-112.
[14] Hernández A. G., Kudriavtsev Yu., Gallardo S., Avendaño M., Asomoza R., (2015), Formation of self–organized nano–surfaces on III–V semiconductors by low energy oxygen ion bombardment. *Mater. Sci. Semiconduct. Process.* 37: 190-198.
[15] Jiang X. F., Weng Q., Wang X. B., Li X., Zhang J., Golberg D., Bando Y., (2015), Recent progresses on fabrications and applications of boron nitride nanomaterials: A Review. *J. Mater. Sci. Technol.* 31: 589-598.
[16] Emanet M., Şen Ö., Çobandede Z., Çulha M., (2015), Interaction of carbohydrate modified boron nitride nanotubes with living cells. *Col. Surf. B.* 134: 440-446.
[17] Ahmad P., Khandaker M. U., Khan Z. R., Amin Y. M., (2015), Synthesis of boron nitride nanotubes via chemical vapor deposition: A comprehensive review. *RSC Adv.* 5: 35116-35137.
[18] Mirzaei M., Mirzaei M., (2011), A computational study of aluminum phosphide nanotubes. *Int. J. Quant. Chem.* 111: 3851-3855.
[19] Wu Q., Hu Z., Wang X., Lu Y., Chen X., Xu H., Chen Y., (2003), Synthesis and characterization of faceted hexagonal aluminum nitride nanotubes. *J. Am. Chem. Soc.* 125: 10176-10177.
[20] Mirzaei M., (2011), A computational NMR study of boron phosphide nanotubes. *Z. Naturforsch. A.* 65: 844-848.
[21] Mirzaei M., Yousefi M., Meskinfam M., (2012), Chemical shielding properties for BN, BP, AlN, and AlP nanocones: DFT studies. *Superlat. Microstruct*. 51: 809–813.
[22] Majidi R., (2015), Electronic properties of T graphene–like C–BN sheets: A density functional theory study. *Physica E* 74: 371-376.
[23] Mansurov V., Malin T., Galitsyn Yu., Zhuravlev K., (2015), Graphene–like AlN layer formation on (111) Si surface by ammonia molecular beam epitaxy. *J. Crys. Growth.* 428: 93-97.
[24] Sohbatzadeh Z., Roknabadi M. R., Shahtahmasebi N., Behdani M., (2015), Spin–dependent transport properties of an armchair boron–phosphide nanoribbon embedded between two graphene nanoribbon electrodes. *Physica E.* 65: 61-67.

[25] Joyce H. J., Gao Q., Tan H. H., Jagadish C., Kim Y., Zou J., Smith L. M., Jackson H. E., Yarrison–Rice J. M., Parkinson P., Johnsto M. B., (2011), III–V semiconductor nanowires for optoelectronic device applications. *Prog. Quant. Elec.* 35: 23-75.

[26] Saidi I, Mejri H., Baira M., Maaref H., (2015), Electronic and transport properties of AlInN/AlN/GaN high electron mobility transistors. *Superlat. Microstruct.* 84: 113-125.

[27] Meyer N., Pirson D., Devillers M., Hermans S., (2013), Particle size effects in selective oxidation of lactose with Pd/h–BN catalysts. *Appl. Catal. A.* 467: 463-473.

[28] Zurek E., Autschbach J., (2004), Density functional calculations of the ^{13}C NMR chemical shifts in (9,0) single–walled carbon nanotubes. *J. Am. Chem. Soc.* 126: 13079-13088.

[29] Drago R. S, (1992). *Physical Methods for Chemists.* Second Ed., New York: Saunders College Publishing.

[30] Bagheri Z., Mirzaei M., Hadipour N. L., Abolhassani M. R., (2008), Density functional theory study of boron nitride nanotubes: Calculations of the N–14 and B–11 nuclear quadrupole resonance parameters. *J. Comput. Theor. Nanosci.* 5: 614-618.

[31] Pyykkö P., (2001), Spectroscopic nuclear quadrupole moments. *Mol. Phys.* 99: 1617-1621.

[32] Frisch M.J., Trucks G.W., Schlegel H.B., (1998). GAUSSIAN 98. Pittsburgh: Gaussian Inc.

[33] Hou S., Shen A., Zhang J., Zhao X., Xue Z., (2004), Ab initio calculations on the open end of single-walled BN nanotubes. *Chem. Phys. Lett.* 393: 179-183.